

Data classification by quantum radial basis function networks

Changpeng Shao*

School of Mathematics, University of Bristol, UK

(Dated: September 11, 2020)

Radial basis function (RBF) network is a third layered neural network that is widely used in function approximation and data classification. Here we propose a quantum model of the RBF network. Similar to the classical case, we still use the radial basis functions as the activation functions. Quantum linear algebraic techniques and coherent states can be applied to implement these functions. Differently, we define the state of the weight as a tensor product of single-qubit states. This gives a simple approach to implement the quantum RBF network in the quantum circuits. Theoretically, we prove that the training is almost quadratic faster than the classical one. Numerically, we demonstrate that the quantum RBF network can solve binary classification problems as good as the classical RBF network. While the time used for training is much shorter.

Neural networks are important approaches in machine learning, which have wide applications in many disciplines [1, 2]. With the developments of quantum techniques, different kinds of generalizations of neural networks have been investigated in the quantum computer [3–10]. One type of neural network has been extensively studied in the quantum case is the feed-forward neural network (or multilayer perceptron). For instance, Beer et al. [3] generalize this by describing the input as a density operator, viewing the unitary and partial trace operations as the activation functions. Killoran et al. [4] consider it in the architecture of continuous-variable quantum computer. In this model, the Gaussian and non-Gaussian gates are used to simulate the key operations of classical neural networks. It can implement nonlinear operations while remaining unitary. Wan et al. [5] make classical neurons implementable in a quantum computer by adding an ancillary qubit. For near-term applications, [6, 7] build feed-forward quantum neural networks using the idea of variational quantum circuits. Another direction is to use quantum linear algebraic techniques to accelerate the efficiency of classical neural networks [11–13]. These works mainly show that the training procedures of certain neural networks can be accelerated in a quantum computer.

In this paper, we will propose a quantum model of the radial basis function (RBF) networks. RBF network was originated from the performing of exact interpolation of a set of data points [14, 15]. It is a shallow linear neural network which has a simple mathematical structure and a relatively cheap training procedure. The network architecture is also similar to the regularization network. From the viewpoint of approximation theory, RBF network can approximate any multivariate continuous function on a compact domain with high accuracy. It has the best-approximation property, and the approximation solution is often optimal. This makes it a popular alternative of multilayer perceptrons. Until now many applications of RBF networks have been found, such as function

approximation [16], data classification [17], time series prediction [18], and the representation of wave function of quantum-mechanical systems [19].

The architecture of an RBF network is simple. It is a type of feed-forward neural network that only has one hidden layer. The activation functions are known as the radial basis function. The output is a linear combination of the training weights and the radial basis functions of the input vectors. RBF network builds on the theorem Cover [20], which states that a complex pattern-classification problem, cast in a high-dimensional space nonlinearly, is more likely to be linearly separable than in a low-dimensional space, provided that the space is not densely populated. Because of this, the input vectors are usually mapped to high dimensional spaces by the radial basis functions. This idea is widely used in the kernel method, in which the radial basis functions play the role of feature maps.

Our quantum generalization of the RBF networks will mainly focus on their ability in data classification. To fit them into the quantum circuits, we will first make some changes to the choices of the weights in the RBF network. Traditionally, in the hidden layer the weights are introduced independently. As Cover’s theorem suggests, if the hidden layer has enough neurons, the classification problem becomes linearly separable. Combining this idea and the requirements of quantum circuits, we define the weight vector as a tensor product of two-dimensional vectors. By doing so, the number of parameters used to determine the weights is exponentially reduced. This also simplifies the implementation of the RBF network in the quantum circuits. We can use the same idea to define an equivalent classical RBF networks. The advantage is that the consuming time used for training is greatly reduced. In the quantum computer, the cost can be further reduced quadratically by the quantum linear algebraic techniques.

The simplification of the structure also brings a disadvantage, i.e. it cannot be used to approximate functions, which is another important application of the traditional RBF network. Based on our experiments, when solving binary classification problems, the performance of the quantum RBF network and the classical RBF network

* changpeng.shao@bristol.ac.uk

are close to each other. But the training time of quantum RBF network is much shorter. When more training samples are involved, the difference becomes more clear. Similar to the classical RBF network, the performance of quantum RBF network increases when more training samples are used during training. Nevertheless, among all the tests, the mean square errors to approximate functions are always large. This implies that the quantum RBF network is not a good function approximator.

The paper is organized as follows: In Section I, we briefly review the design of RBF network and introduce a generalization of this neural network. In Section II, we propose the quantum RBF network and its implementations in quantum circuits. In Section III, we perform numerical experiments to verify the ability of quantum RBF networks in solving classification problems. Finally, in Section IV we present a generalization of the idea to the support vector machines.

I. RADIAL BASIS FUNCTION NETWORK AND ITS GENERALIZATION

A. Radial basis function network

Radial basis function (RBF) network is a type of feed-forward neural network that only has one hidden layer [1, 14]. It builds on the idea of the kernel method. The feature maps used in the RBF network are radial basis functions, which are real-valued functions whose values only depend on the distances between the input vectors and a fixed vector. One typical example is the Gaussian function $\varphi_{c,\sigma}(x) = \exp(-\|x - c\|^2/2\sigma^2)$, where c is a fixed vector and σ is a free parameter. An interesting phenomenon in designing RBF networks is that different choice of the radial basis functions used in the hidden layer have little influence on the performance [21], so we can just focus on the Gaussian functions. It is one of the most commonly used feature maps.

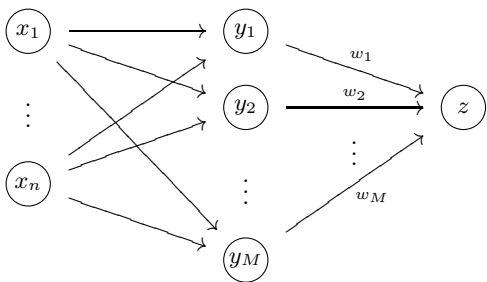


FIG. 1. The structure of RBF network.

The structure of a RBF network is simple, see Figure 1 for an intuition. The input is an n -dimensional real vector $x = (x_1, \dots, x_n)$, e.g. the pixel vector of a picture. In the hidden layer, each $y_i = \varphi_{c_i,\sigma}(x)$ is determined by

a Gaussian function $\varphi_{c_i,\sigma}$. To simplify the design, we use the same σ for all the Gaussian functions. Finally, the output is defined as the linear form $z = \sum_i y_i w_i$ for some weights w_1, \dots, w_M . More generally, we can add a bias b into the network and change the output into $b + \sum_i y_i w_i$.

The training of a RBF network contains two steps. First, determine the parameters used in the Gaussian functions, i.e. the centers c_i and the width σ . A simple choice of the centers is the training samples. More practically, the centers are found by the K -means algorithm. In this setting, the number of weights can be much smaller than the number of training samples. In the second step of training, determine the weights by solving a least-square problem.

For instance, consider the binary classification problem. Suppose we have $M = 2^m$ training samples

$$\{(x^{(t)}, r^{(t)}) \in \mathbb{R}^n \times \{1, -1\} : t = 1, 2, \dots, M\}. \quad (1)$$

If the centers are the training samples, then the feature map is defined by

$$f : \mathbb{R}^n \rightarrow \mathbb{R}^M \\ x \mapsto \left(e^{-\frac{\|x - x^{(1)}\|^2}{2\sigma^2}}, \dots, e^{-\frac{\|x - x^{(M)}\|^2}{2\sigma^2}} \right). \quad (2)$$

Here we choose $\sigma = \max_{r,s} \|x^{(r)} - x^{(s)}\|/\sqrt{2M}$. The weights $w = (w_1, \dots, w_M)$ can be obtained by solving the following least-square problem

$$\min_{w \in \mathbb{R}^M} \tilde{L}(w) = \sum_{t=1}^M \left(f(x^{(t)}) \cdot w - r^{(t)} \right)^2. \quad (3)$$

The training procedure to solve the above least-square problem is time-consuming for a classical computer. The recursive least-square method is often used to reduce the complexity to calculate the matrix inversion. In a quantum computer, quantum linear solvers can be applied to accelerate the solving of (3). This has been recently investigated in [12]. The above is just a brief introduction about the RBF network, for more we refer to [1, 22].

B. A generalization of RBF network

Now we generalize the idea of RBF network from the choices of the weights. The goal is to use this generalization to define a quantum RBF network.

The basic structure is still the same as Figure 1. We only change the weights used in the hidden layer into a tensor product form

$$w(\vec{\theta}) = \bigotimes_{j=1}^m \begin{pmatrix} \cos \theta_j \\ \sin \theta_j \end{pmatrix}, \quad (4)$$

where $m = \lceil \log M \rceil$, and M is the number of training samples. More precisely, let $t = t_1 + t_2 2 + \dots + t_m 2^{m-1}$ be the binary expanding of the integer $t \in \{0, 1, 2, \dots, M - 1\}$.

1}, then it is easy to verify from equation (4) that the t -th weight equals

$$w_t = \prod_{j=1}^m \cos(\theta_j - \frac{t_j \pi}{2}). \quad (5)$$

Even though the dimension of $w(\vec{\theta})$ is M , there are only $\log M$ parameters we need to determine.

As for the training, similar to (3) we need to minimize a loss function

$$L(\vec{\theta}) = \frac{1}{2M} \sum_{t=1}^M \left(f(x^{(t)}) \cdot w(\vec{\theta}) - r^{(t)} \right)^2, \quad (6)$$

where f is defined by equation (2). Since only $\log M$ parameters are need to be determined, the complexity of minimizing L may not as high as minimizing \tilde{L} . Note that L does not define a least-square problem, so we should use general optimization methods like gradient descent or Newton's method to minimize it. About this, we have the following estimation about the cost of each iteration step. We remark that the following result does not consider other potential problems in the gradient descent (e.g. the gradient is zero) and in Newton's method (e.g. the Hessian matrix is singular so that regularization is required). And we will not consider these problems here as our main goal is to design a quantum RBF network.

Theorem 1 *To minimize $L(\vec{\theta})$, if we use the gradient descent method, then the cost of each step of iteration is $O(nM^2)$. If we use the Newton's method, then the cost of each step of iteration is $O(M^2(n + \log^2 M))$.*

Proof. First, assume that the gradient descent method is used. Set the standard basis of \mathbb{R}^m as $\{e_1, \dots, e_m\}$; i.e., e_j is the $\{0, 1\}$ vector such that only the j -th entry equals 1. Then the gradients of L satisfies

$$\nabla L = \frac{1}{M} \sum_{j=1}^m \left(\sum_{t=1}^M \left(w(\vec{\theta}) \cdot f(x^{(t)}) - r^{(t)} \right) \times \frac{\partial w(\vec{\theta})}{\partial \theta_j} \cdot f(x^{(t)}) \right) e_j, \quad (7)$$

By equation (5), the t -th entry of the vector $\partial w(\vec{\theta})/\partial \theta_j$ equals

$$\prod_{i=1}^m \cos(\theta_i - \frac{(t_i - \delta_j^i) \pi}{2}), \quad (8)$$

where δ_j^i is the Kronecker symbol.

We can see that the complexity to compute all $f(x^{(t)})$ is $O(nM^2)$. By equations (5) and (8), the complexity to compute all the entries of $w(\vec{\theta})$, $\partial w(\vec{\theta})/\partial \theta_1, \dots, \partial w(\vec{\theta})/\partial \theta_m$ is $O(m^2 M)$. They are only need to be computed once. After we obtain them, the cost to compute $\sum_{j=1}^m \partial w(\vec{\theta})/\partial \theta_j$ is $O(mM)$. The computation of mM

inner products in equation (7) costs $O(mnM)$. Thus, the total cost to compute ∇L is $O(nM^2 + m^2 M + mnM) = O(nM^2)$.

More advanced optimization methods, such as the Newton's method, are rarely used in machine learning due to the high cost to compute the inverse of the Hessian matrix. However, the Hessian matrix $\nabla^2 L$ of L is m -by- m . So the cost of Newton's method to minimize L is not as high as usual. More precisely, the (j, k) -th entry of $\nabla^2 L$ equals

$$\frac{1}{M} \sum_{t=1}^M \left(w(\vec{\theta}) \cdot f(x^{(t)}) - r^{(t)} \right) \frac{\partial^2 w(\vec{\theta})}{\partial \theta_j \partial \theta_k} \cdot f(x^{(t)}) + \frac{1}{M} \sum_{t=1}^M \left(\frac{\partial w(\vec{\theta})}{\partial \theta_j} \cdot f(x^{(t)}) \right) \left(\frac{\partial w(\vec{\theta})}{\partial \theta_k} \cdot f(x^{(t)}) \right).$$

Similar to the analysis of computing ∇L , the cost to calculate the Hessian matrix of L is $O(m^2 M^2)$. On the other hand, the complexity to compute the inverse of $\nabla^2 L$ is $O(m^3)$. Thus the cost of each iteration of the Newton's method to minimize L is $O(nM^2 + m^2 M^2 + m^3)$. \square

The above result maybe not surprising as we only introduce $m = \log M$ parameters. This will reduce the cost of training but may weaken the power of the RBF network in solving practical problems. In Section III, we will numerically investigate this.

II. QUANTUM RADIAL BASIS FUNCTION NETWORK

Based on the generalization of the RBF network, we now give a definition of the quantum RBF network. Although RBF networks can be used to solve many problems, in the quantum case we only focus on its ability in data classification. For simplicity, we only give an explicit description of the quantum RBF network for solving binary classification problems.

To build a quantum RBF network, there are two problems we need to solve: First, how to encode the data into the quantum circuits? A commonly used strategy is to encode the data into the amplitudes of a quantum state. Here we use the Gaussian kernel to map the samples into a high dimensional space, then prepare the quantum states of those high dimensional vectors. More precisely, for any vector $x \in \mathbb{R}^n$, we define

$$|f(x)\rangle := U_x |0\rangle^{\otimes m} \propto \sum_{t=1}^M \exp\left(-\frac{\|x - x^{(t)}\|^2}{2\sigma^2}\right) |t\rangle, \quad (9)$$

where $\sigma = \max_{r,s} \|x^{(r)} - x^{(s)}\|/\sqrt{2M}$. This step is similar to the feature map (2).

Another problem is how to introduce the training weights. Based on the idea of the kernel method (or Covers theorem), if we map the data into a high dimensional space, the complex nonlinear pattern classification

problem often becomes linearly separable. So we can use linear form to define the weights. In order to implement it efficiently in a quantum computer, we use tensor product to introduce the linear structure on the weights. Thus we define the parameterized unitary as

$$U(\vec{\theta}) = \bigotimes_{j=1}^m \exp(iY\theta_j) = \bigotimes_{j=1}^m \begin{pmatrix} \cos \theta_j & \sin \theta_j \\ -\sin \theta_j & \cos \theta_j \end{pmatrix}, \quad (10)$$

where Y is the Pauli- Y matrix. As a result, the state $|f(x)\rangle$ is transformed into

$$|z\rangle := U(\vec{\theta})|f(x)\rangle = \langle w(\vec{\theta})|f(x)\rangle |0\rangle^{\otimes m} + |0^\perp\rangle^{\otimes m}, \quad (11)$$

where $|0^\perp\rangle^{\otimes m}$ refers to a state that is orthogonal to the first term, and

$$|w(\vec{\theta})\rangle = U^\dagger(\vec{\theta})|0\rangle^{\otimes m} = \bigotimes_{j=1}^m (\cos \theta_j |0\rangle + \sin \theta_j |1\rangle). \quad (12)$$

Finally, we define the output of the quantum RBF network as the amplitude $\langle w(\vec{\theta})|f(x)\rangle$ of $|0\rangle^{\otimes m}$ of $|z\rangle$. It can be estimated by Hadamard test in a quantum computer.

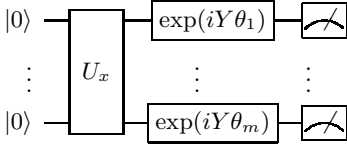


FIG. 2. Quantum circuit of RBF network.

Figure 2 describes the quantum circuit of the quantum RBF network. In the following subsections, we will explain more about how to compute the output by Hadamard test, how to implement U_x and how to train the network.

The structure of the quantum RBF network is the same as the generalized RBF network we defined in Section IB. Because of this, their performance should be close to each other. However, due to the quantum linear algebraic techniques, the calculations in the quantum RBF network can be done much faster. We will show that this speedup is almost quadratic.

A. How to compute the output by measurements?

Generally, for any two real unit vectors x, y , Hadamard test can only extract the information $|\langle x|y\rangle|^2$. A simple technique to overcome this problem is considering $(1, x)$ and $(1, y)$. As for the above-defined quantum RBF network, we can use this idea to extract $\langle w(\vec{\theta})|f(x)\rangle$.

Denote the square of the norm of the vector $f(x)$ as

$$R = \sum_{t=1}^M \exp(-\|x - x^{(t)}\|^2/\sigma^2). \quad (13)$$

Let

$$|\tilde{f}(x)\rangle = \frac{1}{\sqrt{R+1}} (\sqrt{R}|0\rangle|f(x)\rangle + |1\rangle|0\rangle^{\otimes m}). \quad (14)$$

This state is obtained by introducing one extra sample x into (1) as $\exp(-\|x - x\|^2/2\sigma^2) = 1$. To prepare $|\tilde{f}(x)\rangle$, the label of x is not important. Consequently, if we know how to prepare the state $|f(x)\rangle$, then we can similarly prepare $|\tilde{f}(x)\rangle$. This problem is studied in the next subsection.

Now suppose we already have $|\tilde{f}(x)\rangle$. By viewing the first qubit $|0\rangle$ as the control qubit, we can apply $U(\vec{\theta})$ to $|f(x)\rangle$ to create

$$\begin{aligned} & \frac{1}{\sqrt{R+1}} (\sqrt{R}|0\rangle U(\vec{\theta})|f(x)\rangle + |1\rangle|0\rangle^{\otimes m}) \\ &= \frac{1}{\sqrt{R+1}} (\sqrt{R}\langle w(\vec{\theta})|f(x)\rangle |0\rangle|0\rangle^{\otimes m} + |1\rangle|0\rangle^{\otimes m} \\ & \quad + \text{orthogonal terms}). \end{aligned}$$

Apply Hadamard gate to the first qubit, then we obtain

$$\begin{aligned} & \frac{1}{\sqrt{R+1}} \left(\frac{1}{\sqrt{2}} (\sqrt{R}\langle w(\vec{\theta})|f(x)\rangle - 1) |0\rangle^{\otimes (m+1)} \right. \\ & \quad + \frac{1}{\sqrt{2}} (\sqrt{R}\langle w(\vec{\theta})|f(x)\rangle + 1) |1\rangle|0\rangle^{\otimes m} \\ & \quad \left. + \text{orthogonal terms} \right). \end{aligned}$$

Apply amplitude estimation to estimate the amplitudes of $|0\rangle^{\otimes (m+1)}$ and $|1\rangle|0\rangle^{\otimes m}$, we obtain approximations of

$$\frac{1}{2(R+1)} (\sqrt{R}\langle w(\vec{\theta})|f(x)\rangle - 1)^2, \quad (15)$$

$$\frac{1}{2(R+1)} (\sqrt{R}\langle w(\vec{\theta})|f(x)\rangle + 1)^2. \quad (16)$$

The difference of these two approximations gives an approximation of $\langle w(\vec{\theta})|f(x)\rangle$.

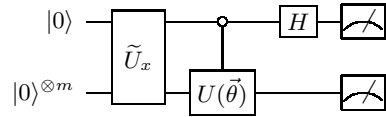


FIG. 3. Quantum circuit to compute the output.

The above procedure is described in Figure 3. In the circuit, H is the Hadamard gate, \tilde{U}_x is used to prepare the state $|\tilde{f}(x)\rangle$.

B. How to implement the unitary U_x ?

The input problem is a bottleneck of many quantum machine learning algorithms. In the design of the quantum RBF network, this is also a constriction. In this

subsection, we will use the idea of coherent states and quantum linear algebraic techniques to implement the unitary U_x in a quantum computer. In the following, we will consider the preparation of the states $|f(x^{(t)})\rangle$ of the training samples. As for the preparation of $|f(x)\rangle$, we can view x as a new sample and prepare the state in the same way.

Coherent states play a crucial role in quantum optics and mathematical physics [23, 24]. They are defined in the Fock states $\{|0\rangle, |1\rangle, \dots\}$, which is a basis of the infinitely dimensional Hilbert space \mathcal{H} . The number n of $|n\rangle$ represents the number of phonons. Let $\mathbf{a}, \mathbf{a}^\dagger$ respectively be the annihilation, creation operator of the harmonic oscillator, then

$$\mathbf{a}|n\rangle = \sqrt{n}|n-1\rangle, \quad \mathbf{a}^\dagger|n\rangle = \sqrt{n+1}|n+1\rangle.$$

For any $n \geq 1$, it is easy to see that

$$|n\rangle = \frac{(\mathbf{a}^\dagger)^n}{\sqrt{n!}}|0\rangle. \quad (17)$$

Let $r \in \mathbb{R}$ be a real number, its coherent state is defined by

$$|\psi_r\rangle = e^{-r^2/2\sigma^2} \sum_{k=0}^{\infty} \frac{(r/\sigma)^k}{\sqrt{k!}} |k\rangle. \quad (18)$$

It is a unit eigenvector of \mathbf{a} corresponding to the eigenvalue r/σ , that is $\mathbf{a}|\psi_r\rangle = (r/\sigma)|\psi_r\rangle$. From (17), we also have $|\psi_r\rangle = e^{-r^2/2\sigma^2} e^{r\mathbf{a}^\dagger/\sigma}|0\rangle = e^{r(\mathbf{a}^\dagger - \mathbf{a})/\sigma}|0\rangle$, thus $|\psi_r\rangle$ is obtained by a unitary operator of dimension infinity.

As for the preparation of $|\psi_r\rangle$ in a finite quantum circuit, we can consider its Taylor approximation:

$$|\tilde{\psi}_r\rangle \propto \sum_{k=0}^{N-1} \frac{(r/\sigma)^k}{\sqrt{k!}} |k\rangle. \quad (19)$$

Before normalization, the error is bounded by

$$\sum_{k=N}^{\infty} \frac{(r/\sigma)^{2k}}{k!} \leq \frac{(r/\sigma)^{2N}}{N!} e^{(r/\sigma)^2}. \quad (20)$$

By Stirling's approximation, $N! \approx \sqrt{2\pi N}(N/e)^N$. Set the upper bound of the error (20) as ϵ , then

$$\log \frac{1}{\epsilon} - \log \sqrt{2\pi} + \frac{r^2}{\sigma^2} \leq (N + \frac{1}{2}) \log N - N(1 + 2 \log \frac{r}{\sigma}).$$

So we can choose $N = O(r^2/\sigma^2 + \log 1/\epsilon)$. With this choice, $\| |\psi_r\rangle - |\tilde{\psi}_r\rangle \|^2 \leq e^{r^2/\sigma^2} \epsilon$. As for the quantum state $|\tilde{\psi}_r\rangle$, it can be prepared in time $O(\log 1/\epsilon)$ by a standard technique [25]. Similar to the Taylor expanding, another method is to truncate the skew-Hermitian matrix $\mathbf{a}^\dagger - \mathbf{a}$ to dimension $O(\log 1/\epsilon)$. This is a 2-sparse matrix, the Hamiltonian simulation is efficient [26]. Therefore, there is an efficient quantum circuit to prepare the coherent state $|\psi_r\rangle$ up to precision ϵ in time $O(\log 1/\epsilon)$.

The coherent state for a real vector $x = (x_1, \dots, x_n)$ is defined by

$$|\psi_x\rangle = |\psi_{x_1}\rangle \otimes \dots \otimes |\psi_{x_n}\rangle. \quad (21)$$

It is not hard to check that for any two real vectors x, y , we have $\langle \psi_x | \psi_y \rangle = \exp(-\|x - y\|^2/2\sigma^2)$.

Now consider the following superposition of coherent states of the training samples:

$$|\Psi\rangle = \frac{1}{\sqrt{M}} \sum_{t=1}^M |t\rangle |\psi_{x^{(t)}}\rangle. \quad (22)$$

This state is obtained by first preparing all the coherent states $|\psi_{x^{(t)}}\rangle$, then generate their superposition by Hadamard transform. Since the error in preparing each state $|\psi_{x^{(t)}}\rangle$ is bounded by $n\epsilon$, to make sure the error of preparing $|\Psi\rangle$ is bounded by δ , we choose $\epsilon = \delta/n$. Consequently, the total cost to prepare $|\Psi\rangle$ is $O(Mn \log 1/\epsilon) = O(Mn \log n/\delta)$.

Taking the partial trace on the second register of $|\Psi\rangle\langle\Psi|$ gives rise to the density operator of the kernel matrix

$$\begin{aligned} \rho &:= \text{Tr}_2 |\Psi\rangle\langle\Psi| \\ &= \frac{1}{M} \sum_{s,t=1}^M \exp(-\|x^{(s)} - x^{(t)}\|^2/2\sigma^2) |s\rangle\langle t|. \end{aligned} \quad (23)$$

As a result,

$$\begin{aligned} \rho|t\rangle &= \frac{1}{M} \sum_{s=1}^M \exp(-\|x^{(s)} - x^{(t)}\|^2/2\sigma^2) |s\rangle \\ &= \frac{\sqrt{R_t}}{M} |f(x^{(t)})\rangle, \end{aligned} \quad (24)$$

where $R_t = \sum_{s=1}^M \exp(-\|x^{(s)} - x^{(t)}\|^2/\sigma^2)$ is the square of the norm of the vector $f(x^{(t)})$. The matrix-vector multiplication (24) can be accomplished by the basic quantum linear algebraic techniques, such as the block-encoding [27]. With the above preliminaries, by Lemma 45 of [27], we can construct an $(1, n + \log M, 0)$ -block-encoding of ρ in cost $O(Mn \log n/\delta)$. As a result, we can create

$$\rho|t\rangle|0\rangle + |0\rangle^\perp \quad (25)$$

at the same time. Note that if we first compute all $\exp(-\|x^{(s)} - x^{(t)}\|^2/2\sigma^2)$, then prepare the quantum states of the samples, the cost is at least $O(M^2)$, which is the same as the complexity of the classical input reading problem. So the above quantum procedure shows that quantum RBF can have a quadratic speedup on M in the input problem.

Certainly, we can perform measurements on the state (25) to get the state $|f(x^{(t)})\rangle$. We can also choose (25) as the result of U_x since we need to do the amplitude estimation at the end of the quantum circuit in Figure 2.

C. How to train the quantum RBF network?

Following the idea of variational quantum eigensolver [28], the training of the quantum RBF network is accomplished by using the quantum-classical hybrid method to minimize the loss function

$$L(\vec{\theta}) = \frac{1}{2M} \sum_{t=1}^M \left(\langle w(\vec{\theta}) | f(x^{(t)}) \rangle - r^{(t)} \right)^2. \quad (26)$$

As discussed in Theorem 1, the costs of gradient descent and Newton's method to minimize $L(\vec{\theta})$ only differ by a logarithmic term at each step of iteration. In the quantum computer, this result should also correct. By the quantum linear algebraic techniques, in a quantum computer the cost of each iteration of these two methods can be reduced quadratically. In the following, we only present an analysis of the gradient descent method to minimize $L(\vec{\theta})$.

When considering the training, based on the algorithm in the above subsection to prepare the quantum states, we can change the quantum circuit shown in Figure 2 into Figure 4 below. Note that in Figure 4, U_{in} does not depend on t , the index of the t -th sample.

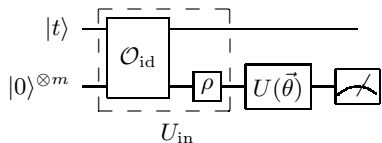


FIG. 4. Quantum circuit of the quantum RBF network, where ρ is the density operator (23) and $O_{\text{id}}|t, 0\rangle = |t, t\rangle$.

In the gradient descent, we update $\vec{\theta}$ via

$$\theta_j = \theta_j - \eta \sum_{t=1}^M \left(\langle w(\vec{\theta}) | f(x^{(t)}) \rangle - r^{(t)} \right) \left\langle \frac{\partial w(\vec{\theta})}{\partial \theta_j} | f(x^{(t)}) \right\rangle, \quad (27)$$

where η is the learning step, $j = 1, 2, \dots, m$. By equations (10) and (12),

$$\begin{aligned} \left\langle \frac{\partial w(\vec{\theta})}{\partial \theta_j} \right\rangle &= \langle 0 |^{\otimes m} \bigotimes_{l=1}^{j-1} \exp(iY\theta_l) \\ &\otimes \exp(iY(\theta_j + \frac{\pi}{2})) \otimes \bigotimes_{l=j+1}^m \exp(iY\theta_l). \end{aligned} \quad (28)$$

Consequently, to estimate $\langle \frac{\partial w(\vec{\theta})}{\partial \theta_j} | f(x^{(t)}) \rangle$, we only need to change the parameter θ_j into $\theta_j + \frac{\pi}{2}$ in Figure 4, then use the amplitude estimation to estimate the amplitude of $|0\rangle^{\otimes m}$.

Now we consider the calculation of the summation in equation (27). Denote the unitary in (28) as $U_j(\vec{\theta})$. For

the first term of the summation, by (24), it equals

$$\langle 0 |^{\otimes m} U(\vec{\theta}) \rho \left(\sum_{t=1}^M \frac{M^2}{R_t} |t\rangle \langle t| \right) \rho U_j(\vec{\theta}) |0\rangle^{\otimes m}. \quad (29)$$

Notice that $U(\vec{\theta}), U_j(\vec{\theta})$ are tensor products of single-qubit gates, ρ can be implemented by quantum linear algebraic techniques (see (25)), and $\sum_{t=1}^M (M^2/R_t) |t\rangle \langle t|$ is a diagonal matrix, the quantity (29) can be estimated to certain precision in time linear on M .

The second term of the summation of (27) equals

$$\langle 0 |^{\otimes m} U_j(\vec{\theta}) \rho \sum_{t=1}^M \frac{Mr^{(t)}}{\sqrt{R_t}} |t\rangle. \quad (30)$$

The quantum state $\sum_{t=1}^M (Mr^{(t)}/\sqrt{R_t}) |t\rangle$ can be prepared by the standard techniques in time $O(M)$. So the quantity (30) can also be computed in time linear at M . Compared to the result of Theorem 1, the training of quantum RBF network is almost quadratic faster than the classical RBF network.

III. NUMERICAL TESTS

To test the performance of the quantum RBF network, we use it to solve binary classification problems in dimension two. However, we only do the experiments for the generalized RBF network defined in Section IB in the classical computer since we do not have a large-scale quantum computer now. Due to the closeness, the testing results should be true for a fault-tolerant quantum computer.

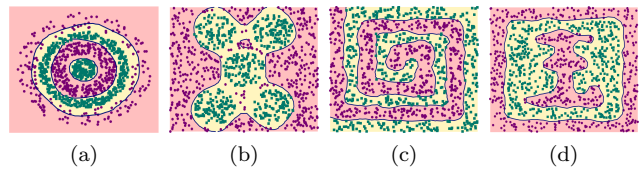


FIG. 5. Use quantum RBF network to solve binary classification problems: 1024 training samples, 10 weight parameters are used.

We tested dozens of examples with different types of classification patterns. In Figure 5, we list four typical testing results. They indicate that the quantum RBF network can solve the binary classification problems with high precision.

Usually, the performance of a machine learning method improves with the increment of training samples. In Figure 6, we consider the influence of the number of training samples on the performance of the quantum RBF network. Note that for classifiers, during training we concern more about the ratio of correct predictions (RCP),

which is defined by

$$\text{RCP} := 1 - \frac{1}{4M} \sum_{t=1}^M \left(\text{sign}(w(\vec{\theta}) \cdot f(x^{(t)})) - r^{(t)} \right)^2. \quad (31)$$

It computes the ratio of training samples that being given the correct labels by the neural network after training. For a classifier, we hope its RCP is large. However, the training is accomplished by minimizing the mean square error (MSE) defined by equation (6). If MSE is small, then this classifier can also be used to approximate functions, that is it can solve regression problems as well.

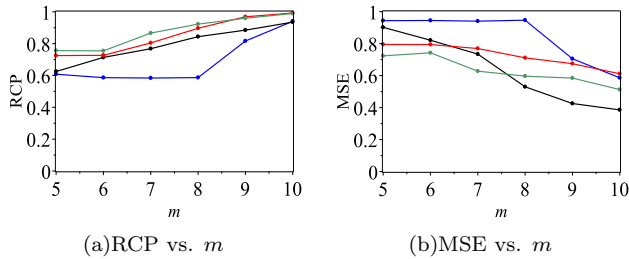


FIG. 6. The influence of the number of training samples on the performance of the quantum RBF network: m is the logarithm of the number of training samples, the blue, black, red and green curves respectively represents the results of pattern (a), (b), (c), (d) in Figure 5.

In Figure 6 we tested all the four patterns of Figure 5. In each situation, we randomly test 10 examples, then compute the average values of the RCPs and MSEs. As we can see from Figure 6(a), the overall trend of RCP is increasing. When using 1024 training samples, the RCPs are all larger than 0.9. This means that the performance of the quantum RBF network to solve classification problems increases when the number of training samples increases. On the other hand, the overall trend of MSE shown in Figure 6(b) is decreasing. However, the MSEs are still large (≥ 0.35) even if we use 1024 training samples. As a result, this kind of neural network seems not a good method to solve regression problems.

Finally, in Table I we compare the performance of the quantum RBF network and the classical RBF network defined in Section IA in solving 10 different classification problems. All the tests are performed on Maple 2019 with command `Minimize` in the package `Optimization`. The processor of the DELL computer is Intel(R) Core(TM) i3-6100 CPU@3.70GHz.

In Table I, INF refers to the ability to do inference on new data after training. It has a similar definition to RCP. In each case, we use M new samples to compute this quantity. The first three have simple patterns, so we just use $M = 256$ training samples. The pattern of the next three are a little complicated, thus $M = 512$ training samples are used. The last four are the four patterns shown in Figure 5, where 1024 training samples are used. In the last four examples, the backslash “/” means that the classical RBF network cannot finish the training after

NO		Time(sec.)	RCP	MSE	INF
1	Q	47.32	0.998	0.465	0.998
	C	72.89	0.992	2.468×10^{-11}	0.996
2	Q	37.78	0.998	0.742	0.992
	C	70.58	0.992	3.906×10^{-15}	0.988
3	Q	56.57	0.953	0.291	0.963
	C	118.42	0.998	4.715×10^{-3}	0.955
4	Q	319.42	0.959	0.567	0.951
	C	3151.39	0.998	2.717×10^{-7}	0.947
5	Q	394.91	0.949	0.231	0.924
	C	3284.71	0.996	4.912×10^{-3}	0.959
6	Q	456.61	0.971	0.686	0.879
	C	3091.18	0.998	2.089×10^{-7}	0.887
7	Q	8025.65	0.941	0.586	0.968
	C	/	/	/	/
8	Q	7951.36	0.935	0.385	0.989
	C	/	/	/	/
9	Q	7365.29	0.992	0.611	0.992
	C	/	/	/	/
10	Q	7133.19	0.989	0.513	0.947
	C	/	/	/	/

TABLE I. Comparison of the performance of the quantum and classical RBF networks. In the second column, Q and C respectively refer to quantum RBF network and the classical RBF network.

10 hours. From the time used in each case, we can train the quantum RBF network much faster than the classical RBF network. The difference becomes more clear when more training samples are used. This is consistent with Theorem 1. When both methods work, the RCP and INF have little difference. This shows that the performance of these two methods in solving classification problems are close to each other. However, the MSEs of the quantum RBF network are always large. So it is not a good method to solve regression problems.

IV. A RELATED IDEA TOWARDS THE SUPPORT VECTOR MACHINES

Support vector machine (SVM) is an important kernel learning method [29]. In this section, we present a generalization of the idea used in RBF network to SVM. This can improve the efficiency of training SVM. But it removes the convex optimization theory of SVM and cannot find the support vectors. So this method is preferable when the computation is an obstacle to SVM.

Consider the binary classification problem discussed in equation (1). Let f be a feature map, then the kernel-based SVM is a method aims to find a hyperplane $f(x) \cdot v - b = 0$ that can separate the two classes with maximal margin. Points on the boundaries $(f(x^{(t)}) \cdot v - b)r^{(t)} = 1$ are called support vectors. The distance from support

vectors to the hyperplane $f(x) \cdot v - b = 0$ equals $1/\|v\|$. Thus SVM reduces to solve the following optimization problem:

$$\begin{aligned} \text{Min} \quad & \frac{1}{2} \|v\|^2 \\ \text{s.t.} \quad & (f(x^{(t)}) \cdot v - b)r^{(t)} \geq 1, \quad t = 1, 2, \dots, M. \end{aligned} \quad (32)$$

Introduce the Lagrangian function

$$L = \frac{1}{2} \|v\|^2 - \sum_{t=1}^M w_t \left((f(x^{(t)}) \cdot v - b)r^{(t)} - 1 \right). \quad (33)$$

Setting the partial derivatives $\partial L/\partial v$ and $\partial L/\partial b$ as zero leads to

$$v = \sum_{t=1}^M w_t r^{(t)} f(x^{(t)}), \quad \sum_{t=1}^M w_t r^{(t)} = 0. \quad (34)$$

Substituting them into equation (32), then we obtain the Lagrangian dual problem of (32) as follows

$$\begin{aligned} \text{Max} \quad Q(w) &= \sum_{t=1}^M w_t - \frac{1}{2} \sum_{s,t=1}^M w_s w_t r^{(s)} r^{(t)} f(x^{(s)}) \cdot f(x^{(t)}), \\ \text{s.t.} \quad & \sum_{t=1}^M w_t r^{(t)} = 0, \quad w_t \geq 0, \quad t = 1, 2, \dots, M. \end{aligned} \quad (35)$$

The solution of the problem (35) is usually sparse, that is $w_t \neq 0$ if $x^{(t)}$ is a support vector. By equation (34), v is a linear combination of the support vectors. The decision boundary is

$$\sum_{x^{(t)}: \text{support vectors}} w_t r^{(t)} f(x^{(t)}) \cdot f(x) - b = 0. \quad (36)$$

The SVM can be described in the language of RBF network. The support vectors are the centers used in the hidden layer, and b is the partial bias. Since we do not know the support vectors in advance, if we simply use all the training samples in equation (36), then the decision boundary is the same as that defined in the RBF network.

However, the approaches to find the weights are different in these two methods.

The advantage of SVM is the convex optimization theory it relies on. This perhaps makes it the most elegant of all kernel-based learning methods. The major limitation of SVM is the fast increase in the computing and storage requirements with respect to the number of training examples. Based on the idea of quantum RBF network, we can change the weight $w = (w_1, \dots, w_M)$ into the tensor product form (4). The advantage of doing so is that only $\log M$ parameters are required. This can save a lot of time to solve the optimization problem. However, it will change the nature of SVM. Moreover, the convex property disappears. Numerical tests show that this method can solve classification problems with high precision (see

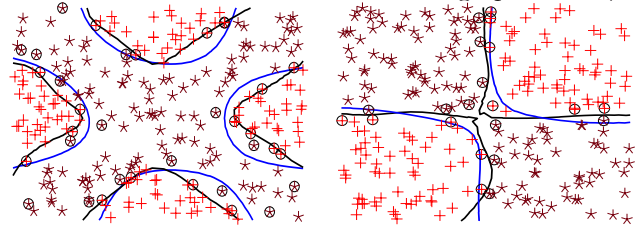


FIG. 7. The black curves are the decision boundaries discovered by the SVM with the usual choice of the weight; the blue ones are obtained by choosing the weight has the form (4). The circles represent the support vectors.

figure 7 for two examples), while it cannot find the support vectors. The solution found by this method is not sparse. This kind of idea is preferable when the training of the SVM is inefficient. When we have a large-scale quantum computer, the efficiency of training can be further improved.

ACKNOWLEDGEMENT

This work was supported by the QuantERA ERA-NET Cofund in Quantum Technologies implemented within the European Union's Horizon 2020 Programme (QuantAlgo project), and EPSRC grants EP/L021005/1 and EP/R043957/1.

-
- [1] S. O. Haykin, *Neural Networks and Learning Machines*, 3rd ed. (Pearson, London, 2008).
 - [2] Y. LeCun, Y. Bengio, and G. Hinton, *nature* **521**, 436 (2015).
 - [3] K. Beer, D. Bondarenko, T. Farrelly, T. J. Osborne, R. Salzmann, D. Scheiermann, and R. Wolf, *Nature communications* **11**, 1 (2020).
 - [4] N. Killoran, T. R. Bromley, J. M. Arrazola, M. Schuld, N. Quesada, and S. Lloyd, *Physical Review Research* **1**, 033063 (2019).
 - [5] K. H. Wan, O. Dahlsten, H. Kristjánsson, R. Gardner, and M. Kim, *npj Quantum Information* **3**, 1 (2017).
 - [6] E. Farhi and H. Neven, *arXiv preprint arXiv:1802.06002* (2018).
 - [7] M. Schuld, A. Bocharov, K. M. Svore, and N. Wiebe, *Physical Review A* **101**, 032308 (2020).
 - [8] C. Shao, *Quantum Information Processing* **19**, 102 (2020).
 - [9] I. Cong, S. Choi, and M. D. Lukin, *Nature Physics* **15**, 1273 (2019).

- [10] G. Verdon, J. Pye, and M. Broughton, arXiv preprint arXiv:1806.09729 (2018).
- [11] I. Kerendis, J. Landman, and A. Prakash, arXiv preprint arXiv:1911.01117 (2019).
- [12] C. Shao, *Quantum Information and Computation* **19**, 0609 (2019).
- [13] P. Rebentrost, T. R. Bromley, C. Weedbrook, and S. Lloyd, *Physical Review A* **98**, 042308 (2018).
- [14] D. S. Broomhead and D. Lowe, *Radial basis functions, multi-variable functional interpolation and adaptive networks*, Tech. Rep. (Royal Signals and Radar Establishment Malvern (United Kingdom), 1988).
- [15] D. Broomhead and D. Lowe, *Complex Systems* **2**, 321 (1988).
- [16] J. Park and I. W. Sandberg, *Neural computation* **3**, 246 (1991).
- [17] R. M. Rifkin, *Everything old is new again: a fresh look at historical approaches in machine learning*, Ph.D. thesis, MIT (2002).
- [18] P. Yee and S. Haykin, *IEEE Transactions on Signal processing* **47**, 2503 (1999).
- [19] P. Teng, *Physical Review E* **98**, 033305 (2018).
- [20] T. M. Cover, *IEEE transactions on electronic computers*, 326 (1965).
- [21] S. Chen, C. F. Cowan, and P. M. Grant, *IEEE Transactions on neural networks* **2**, 302 (1991).
- [22] M. J. Orr, “Introduction to radial basis function networks,” (1996).
- [23] B. C. Sanders, *Journal of Physics A: Mathematical and Theoretical* **45**, 244002 (2012).
- [24] K. Fujii, arXiv preprint quant-ph/0112090 (2001).
- [25] V. V. Shende, S. S. Bullock, and I. L. Markov, *IEEE Transactions on Computer-Aided Design of Integrated Circuits and Systems* **25**, 1000 (2006).
- [26] D. W. Berry, G. Ahokas, R. Cleve, and B. C. Sanders, *Communications in Mathematical Physics* **270**, 359 (2007).
- [27] A. Gilyén, Y. Su, G. H. Low, and N. Wiebe, in *Proceedings of the 51st Annual ACM SIGACT Symposium on Theory of Computing* (2019) pp. 193–204.
- [28] A. Peruzzo, J. McClean, P. Shadbolt, M.-H. Yung, X.-Q. Zhou, P. J. Love, A. Aspuru-Guzik, and J. L. O’Brien, *Nature Communications* **5**, 4213 (2014).
- [29] C. Cortes and V. Vapnik, *Machine learning* **20**, 273 (1995).
- [30] B. Coyle, D. Mills, V. Danos, and E. Kashefi, arXiv preprint arXiv:1904.02214 (2019).
- [31] M. Schuld and N. Killoran, *Physical review letters* **122**, 040504 (2019).